Spatially Modulated Bidirectional Cognitive Cross Network Design With Physical-Layer Coding

Seda Üstünbaş, Ümit Aygölü, and Ertugrul Basar, *Senior Member, IEEE*

***Abstract*—In this paper, a bidirectional cognitive cross network using spatial modulation (SM) along with physical-layer network coding (PLNC) is proposed. In our model, a primary user pair located far from each other, exchanges information in the lack of a direct link so that a relay is required for a reliable communication. A secondary user pair shares their relay with the primary user in return for access to the licensed spectrum. Both users exploit SM while the relay also applies PLNC. It is assumed that each user pair can eavesdrop the signal of the other user pair to use these signals as side information and cancel them from the PLNC mapped signal broadcasted by the relay. Optimum power allocation, in which two scenarios are considered, is proposed for sources and the relay. In *Scenario 1*, the optimization is performed by minimizing the bit error probability (BEP) of the primary user due to its priority in the licensed band. *Scenario 2*, which minimizes BEP of both users, provides the optimum results for the whole system. A theoretical BEP analysis is performed and the results are supported via computer simulation results, which are in perfect match with theoretical findings.**

***Index Terms*—Cognitive radio, spatial modulation, physical-layer network coding.**

I. Introduction

COGNITIVE radio (CR) techniques improve the efficiency of radio resources by allowing unlicensed (*secondary*) users (SUs) to access the frequency bands of licensed (*primary*) users (PUs). SUs can operate in three different modes: underlay, interweave and overlay. In the underlay mode, SUs can access the licensed band provided that the interference created at the primary receiver is below a predefined threshold [1]. In the interweave mode, SUs can find and operate in spectrum vacancies, where PUs are inactive, by using advanced spectrum sensing techniques [2]. In the overlay mode, where cooperative communications has a key role, SUs help PUs to improve the primary performance by realizing spectrum sharing [3].

Physical-layer network coding (PLNC) benefits from the broadcast nature of wireless communications by utilizing interference efficiently instead of avoiding it. Therefore, signal scrambling due to interference is eliminated. Through PLNC, a node can receive signals from different users simultaneously, i.e., with multiple access (MA), and broadcasts (BC) a PLNC mapped symbol generated by the use of exclusive-or (XOR) operation [4], [5]. Two-way relay channels (TWRC), where two nodes exchange information between each other through a relay node, are the simplest structures exploiting PLNC [6].

Spatial modulation (SM), which provides both high spectral and energy efficiencies, is a promising form of multiple-input multiple-output (MIMO) techniques [7]. In SM, the index of the transmit antenna, which is chosen according to the information bits to transmit an M-ary modulated signal in each signaling interval, carries the information along with traditional M-ary modulation schemes. Since only one transmit antenna is activated, only one RF chain is required for transmission, which provides a low-complexity transceiver design and eliminates the need for synchronization among transmit antennas. In addition, SM avoids the inter-channel interference. Due to its inherent advantages, different protocols are considered for SM [8]–[10]. In [8], a differential spatial modulation scheme adopting the denoise-and-forward protocol is proposed for TWRC, which outperforms differential modulation in BER performance due to the provided diversity gain. In [9], adaptive mapper design for SM and a mapper solution, brute forth mapper, which provide the optimal error performance in high signal-to-noise ratio by setting the binary labels of all the closest symbol-pairs, are proposed. In [10], the same authors have proposed a generalized joint 3-D constellation design optimizing the constellation diagram in the complex field, which enhances the transmission reliability of SM. In this study, the authors have compared the proposed method with the existing methods to show its superiority. SM is also considered for both underlay and overlay CR networks [11]–[14]. In [11], an underlay CR network, where secondary transmitter using SM communicates with a secondary receiver by the aid of secondary relays in the presence of multiple PUs, is considered. In [12], adaptive SM is proposed for CR underlay networks in an effort to improve the secondary performance. In [13], a SU transmitter assists the primary network as a relay by using SM to transmit primary and secondary information by traditional modulation schemes and antenna indices, respectively. In [14], an overlay CR cross

Manuscript received October 16, 2017; revised December 22, 2017; accepted March 9, 2018. Date of publication March 14, 2018; date of current version July 16, 2018. This work was supported by the Scientific and Technological Research Council of Turkey (TÜBITAK) under Grant 114E607. The work of E. Basar was supported by the Turkish Academy of Sciences Outstanding Young Scientist Award Programme (TUBA-GEBIP). The review of this paper was coordinated by Dr. C. Yuen. *(Corresponding author: Ertugrul Basar.)*

The authors are with the Electronics and Communication Engineering Department, Istanbul Technical University, Istanbul 34469, Turkey (e-mail: ustunbass@itu.edu.tr; aygolu@itu.edu.tr; basarer@itu.edu.tr).

Digital Object Identifier 10.1109/TVT.2018.2815818

network is proposed, where an SU pair shares its relay with a PU pair to realize spectrum sharing. In this study, it is assumed that the receivers of PU and SU are closer to the transmitter of the other user, while the distances to their own transmitters are too large. Both transmitters and the relay adopt SM to improve the error performance. To the best of our knowledge, the bidirectional cognitive cross network design with optimum power allocation has not been considered yet in the literature.

Against this background, in this paper, a bidirectional cognitive cross network where a PU pair exchanges information by the help of a secondary relay that belongs to a SU pair, is proposed. Since all user pairs are close to the other user pair and far from each other in this model, PU requires a relay for a reliable communication. Therefore, SU shares its relay with PU, in return for access to the licensed spectrum. All nodes apply SM while the relay also uses PLNC along with SM (PLNC-SM). To achieve higher spectral efficiency, a three-time-slot protocol is considered. In this protocol, the nodes of PU (SU) pair send their information bits to the relay node by SM in the first (second) time slot and the relay node applies PLNC to the information bits it received before transmitting this PLNC mapped symbol by SM in the third time slot. Since all nodes receive unintended information along with their intended information from the relay node, they eavesdrop the signals of the nodes belonging to the other user pair to cancel the unintended side information and this leads to the proposed CR cross network design. Furthermore, optimum power allocation (OPA) is also adopted for the relay and the users. Two scenarios are considered for OPA: In *Scenario 1*, optimization is performed by minimizing the bit error probability (BEP) of PU. However, the resulting OPA parameters are not optimum in terms of the whole system performance. Therefore, in *Scenario 2*, optimization is performed to minimize the BEPs of both users. A theoretical BEP analysis is performed and the results are supported via computer simulation results, which are in perfect match with theoretical findings.

Notation: Bold capital and lower case letters denote matrices and vectors, respectively. $\oplus$ denotes bit-wise exclusive-or (XOR) operation. $(.)^H$ stands for Hermitian transpose. The expected value and variance of a random variable (r.v.) X are $\varsigma_X = E[X]$ and $\sigma_X^2 = Var[X]$, respectively. Moment generating function of the r.v. X is $M_X(s) = \int_{-\infty}^{\infty} \exp(sx) f_X(x) dx$, where $f_X(x)$ is the probability density function (pdf) of X.

II. System Model

The considered bidirectional CR cross network is given in Fig. 1, where PU consists of nodes P_1 and P_2 whereas SU includes nodes S_1, S_2 and the relay R. Let us denote the distance between nodes k_i and m by $d_{k_i,m}$, where $k_i \in \{\mathrm{P}_i, \mathrm{S}_i\}, i = 1, 2$ and $m \in \{\mathrm{P}_1, \mathrm{P}_2, \mathrm{R}, \mathrm{S}_1, \mathrm{S}_2\}$. The number of receive antennas at all nodes is denoted by N_r^m while the numbers of transmit antennas at PUs and SUs are denoted by N_t^P and N_t^S, respectively, where the number of transmit antennas are assumed to be equal for P_1 and P_2 as well as for S_1 and S_2. The number of transmit antennas at relay node is $N_t^R = \max(N_t^P, N_t^S)$. $\mathbf{H}^{k_i \to m}$ is the $N_r^m \times N_t^{k_i}$ matrix of channel fading coefficients from node k_i to node m, whose entries are assumed to be zero-mean complex Gaussian r.v.s with variance $d_{k_i,m}^{-v}$, where v is the path-loss exponent. All noise components are assumed to be complex samples of additive white Gaussian noise (AWGN) process with zero mean and unit variance. Total transmission power P_T is equal to the sum of source powers $P_S = P_{\mathrm{P}_1} + P_{\mathrm{P}_2} + P_{\mathrm{S}_1} + P_{\mathrm{S}_2}$ and the power of the relay P_{R} as $P_T = P_S + P_{\mathrm{R}}$, where $P_{\mathrm{P}_1}, P_{\mathrm{P}_2}, P_{\mathrm{S}_1}$ and P_{S_2} are the transmission powers of $\mathrm{P}_1, \mathrm{P}_2, \mathrm{S}_1$ and S_2, respectively. Power allocation factor is defined as $\beta = P_S/P_T$, which means that a power βP_T is allocated to the sources and $(1-\beta)P_T$ to the relay. The powers of αP_S and $(1-\alpha)P_S$ are destined to the primary and secondary users, respectively, i.e., $P_{\mathrm{P}_1} = P_{\mathrm{P}_2} = \alpha P_S/2$ and $P_{\mathrm{S}_1} = P_{\mathrm{S}_2} = (1-\alpha)P_S/2$.

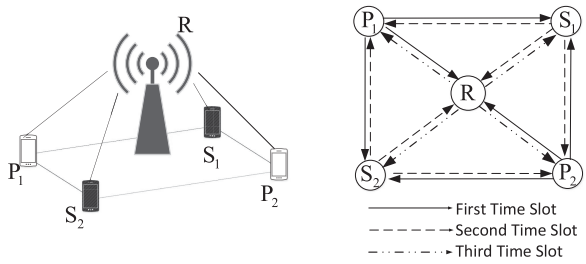

Fig. 1. Considered bidirectional cognitive cross network

The whole transmission of all nodes is completed in three time slots, which is minimum for half-duplex operating nodes [5]. At the first time slot, P_1 and P_2 simultaneously transmit their SM symbols $z_{k_i} = (\ell_{k_i}, x_{k_i})$ to the relay, where ℓ_{k_i} and x_{k_i} denote the active antenna index and the modulated symbol from an M_P-PSK constellation, for the node $k_i = \mathrm{P}_i, i = 1, 2$, respectively. SU's nodes S_1 and S_2 eavesdrop the transmitted SM signals to utilize them as the side information. At the second time slot, similarly, S_1 and S_2 simultaneously transmit their own information bits through SM symbols $z_{k_i} = (\ell_{k_i}, x_{k_i})$ to R, where x_{k_i} is the modulated symbol from an M_S-PSK constellation and $k_i = \mathrm{S}_i, i = 1, 2$. During this time slot, PU's nodes P_1 and P_2 eavesdrop the secondary nodes' transmission to acquire the side information. The received signal vectors at node m are given for the qth time slot as

$$\mathbf{y}_m^{(q)} = \sum_{i=1}^{2} \sqrt{P_{k_i}} \mathbf{h}_{\ell_{k_i}}^{k_i \to m} x_{k_i} + \mathbf{n}_m^{(q)} \tag{1}$$

where $\mathbf{h}_{\ell_{k_i}}^{k_i \to m}$ is the ℓ_{k_i} th column of $\mathbf{H}^{k_i \to m}$. In (1), $q = 1, k_i = \mathrm{P}_i$ and $m \in \{\mathrm{S}_1, \mathrm{S}_2, \mathrm{R}\}$ for the first time slot, while $q = 2$, $k_i = \mathrm{S}_i$ and $m \in \{\mathrm{P}_1, \mathrm{P}_2, \mathrm{R}\}$ for the second time slot. $\mathbf{n}_m^{(q)}$ stands for the vector of noise samples at node m for the qth

TABLE I
CALCULATION OF INTENDED INFORMATION AT DESTINATION NODES

State	P_1	P_2	S_1	S_2	R
$q=1$	Tx: z_{P_1}	Tx: z_{P_2}	Rx: $\hat{z}^{\mathrm{S}_1}_{\mathrm{P}_1}, \hat{z}^{\mathrm{S}_1}_{\mathrm{P}_2}$	Rx: $\hat{z}^{\mathrm{S}_2}_{\mathrm{P}_1}, \hat{z}^{\mathrm{S}_2}_{\mathrm{P}_2}$	Rx: $\hat{z}^{\mathrm{R}}_{\mathrm{P}_1}, \hat{z}^{\mathrm{R}}_{\mathrm{P}_2}$
$q=2$	Rx: $\hat{z}^{\mathrm{P}_1}_{\mathrm{S}_1}, \hat{z}^{\mathrm{P}_1}_{\mathrm{S}_2}$	Rx: $\hat{z}^{\mathrm{P}_2}_{\mathrm{S}_1}, \hat{z}^{\mathrm{P}_2}_{\mathrm{S}_2}$	Tx: z_{S_1}	Tx: z_{S_2}	Rx: $\hat{z}^{\mathrm{R}}_{\mathrm{S}_1}, \hat{z}^{\mathrm{R}}_{\mathrm{S}_2}$
PLNC Symbols	$\bar{z}_{\mathrm{P}_1} = \hat{z}^{\mathrm{P}_1}_{\mathrm{S}_1} \oplus \hat{z}^{\mathrm{P}_1}_{\mathrm{S}_2}$	$\bar{z}_{\mathrm{P}_2} = \hat{z}^{\mathrm{P}_2}_{\mathrm{S}_1} \oplus \hat{z}^{\mathrm{P}_2}_{\mathrm{S}_2}$	$\bar{z}_{\mathrm{S}_1} = \hat{z}^{\mathrm{S}_1}_{\mathrm{P}_1} \oplus \hat{z}^{\mathrm{S}_1}_{\mathrm{P}_2}$	$\bar{z}_{\mathrm{S}_2} = \hat{z}^{\mathrm{S}_2}_{\mathrm{P}_1} \oplus \hat{z}^{\mathrm{S}_2}_{\mathrm{P}_2}$	$\bar{z}_{\mathrm{R}} = \hat{z}^{\mathrm{R}}_{\mathrm{P}_1} \oplus \hat{z}^{\mathrm{R}}_{\mathrm{P}_2} \oplus \hat{z}^{\mathrm{R}}_{\mathrm{S}_1} \oplus \hat{z}^{\mathrm{R}}_{\mathrm{S}_2}$
$q=3$	Rx: $\hat{\bar{z}}^{\mathrm{P}_1}_{\mathrm{R}}$	Rx: $\hat{\bar{z}}^{\mathrm{P}_2}_{\mathrm{R}}$	Rx: $\hat{\bar{z}}^{\mathrm{S}_1}_{\mathrm{R}}$	Rx: $\hat{\bar{z}}^{\mathrm{S}_2}_{\mathrm{R}}$	Tx: $\bar{z}_{\mathrm{R}}$
Intended Information	$\hat{z}_{\mathrm{P}_2} = z_{\mathrm{P}_1} \oplus \bar{z}_{\mathrm{P}_1} \oplus \hat{\bar{z}}^{\mathrm{P}_1}_{\mathrm{R}}$	$\hat{z}_{\mathrm{P}_1} = z_{\mathrm{P}_2} \oplus \bar{z}_{\mathrm{P}_2} \oplus \hat{\bar{z}}^{\mathrm{P}_2}_{\mathrm{R}}$	$\hat{z}_{\mathrm{S}_2} = z_{\mathrm{S}_1} \oplus \bar{z}_{\mathrm{S}_1} \oplus \hat{\bar{z}}^{\mathrm{S}_1}_{\mathrm{R}}$	$\hat{z}_{\mathrm{S}_1} = z_{\mathrm{S}_2} \oplus \bar{z}_{\mathrm{S}_2} \oplus \hat{\bar{z}}^{\mathrm{S}_2}_{\mathrm{R}}$	–

time slot. Maximum likelihood (ML) detection is performed at node $m \in \{\mathrm{S}_1, \mathrm{S}_2, \mathrm{R}\}$ at the first time slot as,

$$(\hat{z}^m_{\mathrm{P}_1}, \hat{z}^m_{\mathrm{P}_2}) = \underset{\ell_{\mathrm{P}_1}, x_{\mathrm{P}_1}, \ell_{\mathrm{P}_2}, x_{\mathrm{P}_2}}{\arg\min} \left\| \mathbf{y}^{(1)}_m - \sum_{i=1}^{2} \sqrt{P_{\mathrm{P}_i}} \mathbf{h}^{\mathrm{P}_i \to m}_{\ell_{\mathrm{P}_i}} x_{\mathrm{P}_i} \right\|^2. \quad (2)$$

At the second time slot, ML detection is performed at node $m \in \{\mathrm{P}_1, \mathrm{P}_2, \mathrm{R}\}$ as,

$$(\hat{z}^m_{\mathrm{S}_1}, \hat{z}^m_{\mathrm{S}_2}) = \underset{\ell_{\mathrm{S}_1}, x_{\mathrm{S}_1}, \ell_{\mathrm{S}_2}, x_{\mathrm{S}_2}}{\arg\min} \left\| \mathbf{y}^{(2)}_m - \sum_{i=1}^{2} \sqrt{P_{\mathrm{S}_i}} \mathbf{h}^{\mathrm{S}_i \to m}_{\ell_{\mathrm{S}_i}} x_{\mathrm{S}_i} \right\|^2. \quad (3)$$

Then, the PLNC mapped SM symbols are generated at nodes $m \in \{\mathrm{P}_1, \mathrm{P}_2, \mathrm{S}_1, \mathrm{S}_2\}$ as $\bar{z}_m = (\bar{\ell}_m, \bar{x}_m)$ by applying bit-wise XOR operation to the binary correspondings of $(\hat{\ell}^m_{k_1}, \hat{x}^m_{k_1})$ and $(\hat{\ell}^m_{k_2}, \hat{x}^m_{k_2})$, which are enrolled as the side information at node m except for R. A PLNC mapped SM symbol $\bar{z}_{\mathrm{R}} = (\bar{\ell}_{\mathrm{R}}, \bar{x}_{\mathrm{R}})$ is generated by applying bit-wise XOR operation to the binary correspondings of $\hat{z}^{\mathrm{R}}_{\mathrm{P}_1}, \hat{z}^{\mathrm{R}}_{\mathrm{P}_2}, \hat{z}^{\mathrm{R}}_{\mathrm{S}_1}$ and $\hat{z}^{\mathrm{R}}_{\mathrm{S}_2}$ at R.

At the third time slot ($q=3$), R broadcasts $\bar{z}_{\mathrm{R}} = (\bar{\ell}_{\mathrm{R}}, \bar{x}_{\mathrm{R}})$ to all nodes. The received signal vector at node m is given by

$$\mathbf{y}^{(3)}_m = \sqrt{P_{\mathrm{R}}} \mathbf{h}^{\mathrm{R} \to m}_{\bar{\ell}_{\mathrm{R}}} \bar{x}_{\mathrm{R}} + \mathbf{n}^{(3)}_m \quad (4)$$

where $m \in \{\mathrm{P}_1, \mathrm{P}_2, \mathrm{S}_1, \mathrm{S}_2\}$ and $\mathbf{h}^{\mathrm{R} \to m}_{\bar{\ell}_{\mathrm{R}}}$ is the $\bar{\ell}_{\mathrm{R}}$th column of $\mathbf{H}^{\mathrm{R} \to m}$. ML detection is performed at node m as

$$(\hat{\bar{\ell}}^m_{\mathrm{R}}, \hat{\bar{x}}^m_{\mathrm{R}}) = \underset{\bar{\ell}_{\mathrm{R}}, \bar{x}_{\mathrm{R}}}{\arg\min} \|\mathbf{y}^{(3)}_m - \sqrt{P_{\mathrm{R}}} \mathbf{h}^{\mathrm{R} \to m}_{\bar{\ell}_{\mathrm{R}}} \bar{x}_{\mathrm{R}}\|^2. \quad (5)$$

Finally, all destination nodes apply bit-wise XOR operation to the binary correspondings of their own information, the side information and the PLNC mapped SM signal detected from (5), to access the intended information. A table for the intended information at destination nodes is provided in Table I.

III. BIT ERROR PERFORMANCE ANALYSIS

In this section, analytical expressions are derived for the BEPs of PU and SU. At the first and second time slots, i.e., $q = 1, 2$, multiple access channels (MAC) occur at all receiving nodes since they receive simultaneously two signals from two other nodes. At the third time slot, i.e., $q = 3$, only R broadcasts a PLNC mapped SM symbol to all other nodes, which forms a broadcast channel (BC). Therefore, in the following sections, BEPs of MAC and BC are considered for the generic case.

A. BEP of Multiple Access Channel

When two different SM symbols are received by a node, BEP of this MAC is derived as follows: From (2) and (3), the decision metric is written as $\Lambda(\ell_{k_i}, x_{k_i}) = \|\mathbf{y}^{(q)}_m - \sum_{i=1}^{2} \sqrt{P_{k_i}} \mathbf{h}^{k_i \to m}_{\ell_{k_i}} x_{k_i}\|^2$, $k_i \in \{\mathrm{P}_i, \mathrm{S}_i\}$ and $q = 1, 2$, then the conditional pairwise error probability (CPEP) is obtained as

$$\begin{aligned} P(\Lambda(\ell_{k_i}, x_{k_i}) \geq \Lambda(\hat{\ell}^m_{k_i}, \hat{x}^m_{k_i}) | \mathbf{H}^{k_1 \to m}, \mathbf{H}^{k_2 \to m}) \\ = P(D \geq 0 | \mathbf{H}^{k_1 \to m}, \mathbf{H}^{k_2 \to m}) \end{aligned} \quad (6)$$

with the decision variable D given by

$$\begin{aligned} D = &-\gamma_{MAC} \\ &- 2\Re \left\{ \mathbf{n}^H_m \left(\sum_{i=1}^{2} \sqrt{P_{k_i}} \left(\mathbf{h}^{k_i \to m}_{\ell_{k_i}} x_{k_i} - \mathbf{h}^{k_i \to m}_{\hat{\ell}^m_{k_i}} \hat{x}^m_{k_i} \right) \right) \right\} \end{aligned}$$

where $\gamma_{MAC} = \| \sum_{i=1}^{2} \sqrt{P_{k_i}} (\mathbf{h}^{k_i \to m}_{\ell_{k_i}} x_{k_i} - \mathbf{h}^{k_i \to m}_{\hat{\ell}^m_{k_i}} \hat{x}^m_{k_i}) \|^2$ and q, k_i and m are as indicated in the paragraph below (1). The expected value and variance of D are given as $\varsigma_D = -\gamma_{MAC}$ and $\sigma^2_D = 2\gamma_{MAC}$, respectively. Then, (6) is calculated by

$$\begin{aligned} P(D \geq 0 | \mathbf{H}^{k_1 \to m}, \mathbf{H}^{k_2 \to m}) &= Q\left(-\frac{\varsigma_D}{\sigma_D} \right) \\ &= \frac{1}{\pi} \int_0^{\pi/2} \exp\left(-\frac{\gamma_{MAC}}{4 \sin^2 \theta} \right) d\theta. \end{aligned} \quad (7)$$

Average pairwise error probability (APEP) is derived by taking the expectation of (7) over the matrices of channel fading coefficients as

$$\begin{aligned} \mathrm{APEP}^{\mathrm{MAC}} = P(D \geq 0) &= \frac{1}{\pi} \int_0^{\pi/2} M_{\gamma_{MAC}} \left(\frac{-1}{4 \sin^2 \theta} \right) d\theta \\ &= \frac{1}{\pi} \int_0^{\pi/2} \left(\frac{\sin^2 \theta}{\sin^2 \theta + \Omega/4} \right)^{N^m_r} d\theta \end{aligned} \quad (8)$$

where Ω is given in the top of next page in (9).

$$\Omega = \begin{cases} P_{k_1} d_{k_1,m}^{-v} |x_{k_1} - \hat{x}_{k_1}^m|^2 + P_{k_2} d_{k_2,m}^{-v} |x_{k_2} - \hat{x}_{k_2}^m|^2, & \ell_{k_1} = \hat{\ell}_{k_1}^m \text{ and } \ell_{k_2} = \hat{\ell}_{k_2}^m \\ P_{k_1} d_{k_1,m}^{-v} |x_{k_1} - \hat{x}_{k_1}^m|^2 + P_{k_2} d_{k_2,m}^{-v} (|x_{k_2}|^2 + |\hat{x}_{k_2}^m|^2), & \ell_{k_1} = \hat{\ell}_{k_1}^m \text{ and } \ell_{k_2} \neq \hat{\ell}_{k_2}^m \\ P_{k_1} d_{k_1,m}^{-v} (|x_{k_1}|^2 + |\hat{x}_{k_1}^m|^2) + P_{k_2} d_{k_2,m}^{-v} |x_{k_2} - \hat{x}_{k_2}^m|^2, & \ell_{k_1} \neq \hat{\ell}_{k_1}^m \text{ and } \ell_{k_2} = \hat{\ell}_{k_2}^m \\ P_{k_1} d_{k_1,m}^{-v} (|x_{k_1}|^2 + |\hat{x}_{k_1}^m|^2) + P_{k_2} d_{k_2,m}^{-v} (|x_{k_2}|^2 + |\hat{x}_{k_2}^m|^2), & \ell_{k_1} \neq \hat{\ell}_{k_1}^m \text{ and } \ell_{k_2} \neq \hat{\ell}_{k_2}^m \end{cases}. \quad (9)$$

The closed form of (8) is given as [15]

$$\text{APEP}^{\text{MAC}} = \frac{1}{2}\left[1 - \mu\left(\frac{\Omega}{4}\right) \sum_{j=0}^{N_r^m - 1} \binom{2j}{j} \left(\frac{1 - \mu^2\left(\frac{\Omega}{4}\right)}{4}\right)^j\right] \quad (10)$$

where $\mu(c) = \sqrt{c/(1+c)}$. Finally, BEP of MAC is upper bounded by

$$P_b^{MAC} \leq \frac{1}{(MN_t)^2} \sum_{z_{k_1}} \sum_{\hat{z}_{k_1}^m} \sum_{z_{k_2}} \sum_{\hat{z}_{k_2}^m} \text{APEP}^{\text{MAC}} \frac{n(z_m, \bar{z}_m)}{\log_2(MN_t)} \quad (11)$$

where $M = M_P$ and $N_t = N_t^P$ when PUs transmitted, $M = M_S$ and $N_t = N_t^S$ when SUs transmitted. In (11) $n(z_m, \bar{z}_m)$ represents the number of erroneous bits in detection of the PLNC mapped SM symbol z_m, when it is decided as $\bar{z}_m$ at node m. Note that an error occurs, if the PLNC mapped SM symbol z_m, which is obtained by applying XOR operation to the binary correspondings of z_{k_1} and z_{k_2}, is different from the PLNC mapped SM symbol $\bar{z}_m$ detected at node m, which is obtained by applying XOR operation to the binary correspondings of $\hat{z}_{k_1}^m$ and $\hat{z}_{k_2}^m$.

B. BEP of Broadcast Channel

When R broadcasts the PLNC mapped SM symbol to node m, BEP of BC is derived by similar steps to that of MAC given in the previous section as follows: From (5), the decision metric is given by $\Lambda(\bar{\ell}_{\text{R}}, \bar{x}_{\text{R}}) = \|\mathbf{y}_m^{(3)} - \sqrt{P_{\text{R}}}\mathbf{h}_{\bar{\ell}_{\text{R}}}^{\text{R}\to m} \bar{x}_{\text{R}}\|^2$. CPEP can be expressed as

$$P\left(\Lambda\left(\bar{\ell}_{\text{R}}, \bar{x}_{\text{R}}\right) \geq \Lambda\left(\hat{\bar{\ell}}_{\text{R}}^m, \hat{\bar{x}}_{\text{R}}^m\right) | \mathbf{H}^{\text{R}\to m}\right) = P\left(D \geq 0 | \mathbf{H}^{\text{R}\to m}\right) \quad (12)$$

where

$$D = -\gamma_{BC} - 2\Re\left\{\mathbf{n}_m^H \left(\sqrt{P_{\text{R}}}\left(\mathbf{h}_{\bar{\ell}_{\text{R}}}^{\text{R}\to m} \bar{x}_{\text{R}} - \mathbf{h}_{\hat{\bar{\ell}}_{\text{R}}^m}^{\text{R}\to m} \hat{\bar{x}}_{\text{R}}^m\right)\right)\right\} \quad (13)$$

where $\gamma_{BC} = ||\sqrt{P_{\text{R}}}(\mathbf{h}_{\bar{\ell}_{\text{R}}}^{\text{R}\to m} \bar{x}_{\text{R}} - \mathbf{h}_{\hat{\bar{\ell}}_{\text{R}}^m}^{\text{R}\to m} \hat{\bar{x}}_{\text{R}}^m)||^2$. The expected value and variance of D are calculated from (13) and CPEP is obtained by

$$P(D \geq 0 | \mathbf{H}^{\text{R}\to m}) = \frac{1}{\pi} \int_0^{\pi/2} \exp\left(-\frac{\gamma_{BC}}{4\sin^2\theta}\right) d\theta. \quad (14)$$

APEP of BC is obtained as in (10). However, in this case, $\Omega = P_{\text{R}}|\bar{x}_{\text{R}} - \hat{\bar{x}}_{\text{R}}^m|^2$ if $\bar{\ell}_{\text{R}} = \hat{\bar{\ell}}_{\text{R}}^m$, $\Omega = P_{\text{R}}(|\bar{x}_{\text{R}}|^2 + |\hat{\bar{x}}_{\text{R}}^m|^2)$ else. Then, BEP of BC is upper bounded by

$$P_b^{BC} \leq \frac{1}{MN_t} \sum_{\bar{z}_{\text{R}}} \sum_{\hat{\bar{z}}_{\text{R}}^m} \text{APEP}^{\text{BC}} \frac{n(\bar{z}_{\text{R}}, \hat{\bar{z}}_{\text{R}}^m)}{\log_2(MN_t)} \quad (15)$$

where $M = \max(M_P, M_S)$, $N_t = \max(N_t^P, N_t^S)$ and $n(\bar{z}_{\text{R}}, \hat{\bar{z}}_{\text{R}}^m)$ represent the number of erroneously detected bits of the SM symbol at node m.

C. End-to-End BEP

Finally, BEP at each end node $m \in \{\text{P}_1, \text{P}_2, \text{S}_1, \text{S}_2\}$ is upper bounded by

$$P_b^m \leq 1 - \Big[\left(1 - P_b^{MAC_1\to R}\right)\left(1 - P_b^{MAC_2\to R}\right) \times \left(1 - P_b^{MAC\to m}\right)\left(1 - P_b^{R\to m}\right)\Big] \quad (16)$$

where $P_b^{MAC_1\to R}$ and $P_b^{MAC_2\to R}$ are BEPs of MAC at R for the first and second time slots, respectively, while $P_b^{MAC\to m}$ is the BEP of MAC at node m and $P_b^{R\to m}$ is the BEP of BC from R to node m, which are calculated from Sections III-A and III-B.

D. Complexity Analysis at the Relay Node

To calculate the receiver complexity of the relay node, we consider the number of the real multiplications [16] performed during the maximum likelihood (ML) detection by (2) and (3), which are equivalent in terms of computational complexity. (2) and (3) can be rewritten as $\sum_{k=1}^{N_r^{\text{R}}} |y(k) - \sqrt{P}(h_{\ell_1}(k)x_1 + h_{\ell_2}(k)x_2)|^2$ for $\ell_1, \ell_2 \in \{1, 2, \ldots, N_t\}$. Here $h_{\ell_i}(k)x_i$ requires a complex multiplication, which is equivalent to 4 real multiplications. Another 2 operations is required to evaluate the squared absolute value. These operations are repeated for $N_r^{\text{R}} \times 2^{\log_2 M^2 N_t^2}$, therefore, the total computational complexity at the relay node is given as $10N_r^{\text{R}} 2^{\log_2 M^2 N_t^2}$.

IV. Optimum Power Allocation

Two scenarios are considered for OPA: *Scenario 1* for which the optimization is performed to minimize BEP of PU, which has priority and *Scenario 2* to minimize the total BEP of both users.

In *Scenario 1*, the convex objective function $\mathcal{F}_1$ is taken as the average of $P_b^{\text{P}_1}$ and $P_b^{\text{P}_2}$ to provide priority for PU. The minimization problem is given as follows:

$$\left(\beta_0^1, \alpha_0^1\right) = \min_{\beta,\alpha} \quad \mathcal{F}_1 = \min_{\beta,\alpha} \quad \left\{0.5\left(P_b^{\text{P}_1} + P_b^{\text{P}_2}\right)\right\}. \quad (17)$$

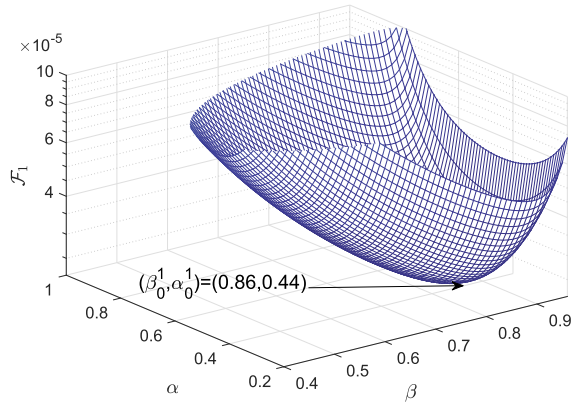

Fig. 2. Meshgrid of *Scenario 1* for $M_P = M_S = N_t^P = N_t^S = 4$.

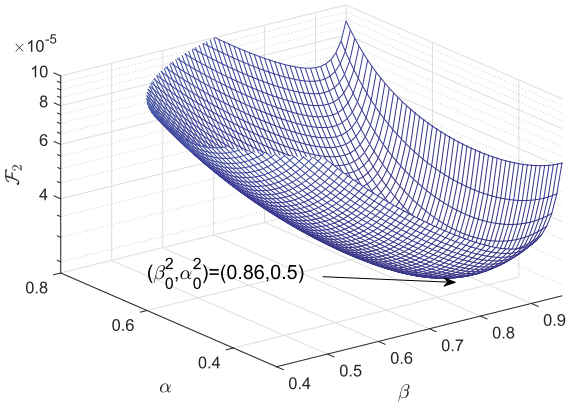

Fig. 3. Meshgrid of *Scenario 2* for $M_P = M_S = N_t^P = N_t^S = 4$.

The optimal pair (β_0^1, α_0^1) for PU is not the optimal solution for the whole system performance. Since PU has the priority in the licensed spectrum, performance of SU, which degrades in this case, is not taken into account. Therefore, another convex objective function is considered in *Scenario 2*.

In *Scenario 2*, optimization is performed by minimizing the sum BEP of both users, which is obtained by averaging the total BEP of end nodes as

$$\left(\beta_0^2, \alpha_0^2\right) = \min_{\beta,\alpha} \mathcal{F}_2 = \min_{\beta,\alpha} 0.25 \left(P_b^{\mathrm{P}_1} + P_b^{\mathrm{P}_2} + P_b^{\mathrm{S}_1} + P_b^{\mathrm{S}_2}\right). \tag{18}$$

For both scenarios, it is very difficult to obtain an analytical solution for the above power allocation problem due to the complicated mathematical steps involving several power allocation parameters. Hence, numerical optimization is applied.

V. Performance Evaluation

In this section, theoretical BEPs derived in Section III are compared with computer simulation results for $v = 4$ and $N_r^m = 2$. The effects of M_P, N_t^P, M_S, N_t^S and the relay position on the BEP performance of PU and SU are investigated and the performance of PU is compared with that of the direct transmission in the absence of SU. OPA parameters are numerically obtained for both scenarios in the next section.

A. Optimum Power Allocation

OPA parameters (β_0^1, α_0^1) and (β_0^2, α_0^2) for *Scenario 1* and *2*, respectively, are obtained as follows: β and α in $\mathcal{F}_1$ and $\mathcal{F}_2$ are varied in the interval $0 < \beta, \alpha \leq 0.99$ by the step size 0.01 and the pair (β, α), which gives the minimum value of the convex objective function is chosen for each scenario.

In Figs. 2 and 3, the convex objective functions $\mathcal{F}_1$ and $\mathcal{F}_2$ of (17) and (18), respectively, are given in 3-D plane for $M_P = M_S = 4, N_t^P = N_t^S = 4$ and $P_T = 40$ dB when unit distance is assumed between every node pair. In Fig. 2 for *Scenario 1*, more power is allocated to SU to improve the BEP performance of four links, which convey side information to P_1 and P_2 from S_1 and S_2. However, this degrades the BEP performance of SU. In Fig. 3 for *Scenario 2*, the BEP of the whole system is minimized by increasing α compared to its value in *Scenario 1*, i.e., $\alpha_0^1 < \alpha_0^2$. In the case where all links have unit distance, OPA parameters for different settings of modulation orders and the numbers of transmit antennas are given in Table II, for both scenarios, when $P_T = 40$ dB. As the spectral efficiency increases, so does β. Therefore, more power is allocated to the sources compared to R. The effect of relay position is investigated in Table III for $M_P = M_S = N_t^P = N_t^S = 4$ and $P_T = 40$ dB, where R is assumed on the same plane as $\mathrm{P}_1, \mathrm{P}_2, \mathrm{S}_1, \mathrm{S}_2$ and when R moves on the vertical direction from the midst of P_1 and S_1 to the midst of P_2 and S_2. From this table, we conclude that more power is allocated to the sources when R is equidistant to four sources. However, as R moves to the midst of P_1 and S_1 or the opposite side, R requires more power.

TABLE II
Parameters (β_0, α_0) When All Distances Are Unit

M_P	N_t^P	M_S	N_t^S	*Scenario1*	*Scenario 2*
2	2	2	2	(0.83, 0.44)	(0.83, 0.5)
2	4	2	4	(0.84, 0.44)	(0.84, 0.5)
4	4	4	4	(0.86, 0.44)	(0.86, 0.5)
2	8	2	8	(0.86, 0.44)	(0.86, 0.5)
4	8	4	8	(0.88, 0.44)	(0.88, 0.5)
4	16	4	16	(0.90, 0.44)	(0.90, 0.5)

TABLE III
Effect of Relay Position on (β_0, α_0) for $M_P = M_S = N_t^P = N_t^S = 4$

$d_{\mathrm{R,P_1}}$	$d_{\mathrm{R,P_2}}$	$d_{\mathrm{R,S_1}}$	$d_{\mathrm{R,S_2}}$	*Scenario 1*	*Scenario 2*
$\sqrt{2}/2$	$\sqrt{2}/2$	$\sqrt{2}/2$	$\sqrt{2}/2$	(0.91, 0.28)	(0.92, 0.5)
$1/2$	$\sqrt{5}/2$	$1/2$	$\sqrt{5}/2$	(0.83, 0.4)	(0.84, 0.5)
$\sqrt{5}/2$	$1/2$	$\sqrt{5}/2$	$1/2$	(0.83, 0.4)	(0.84, 0.5)

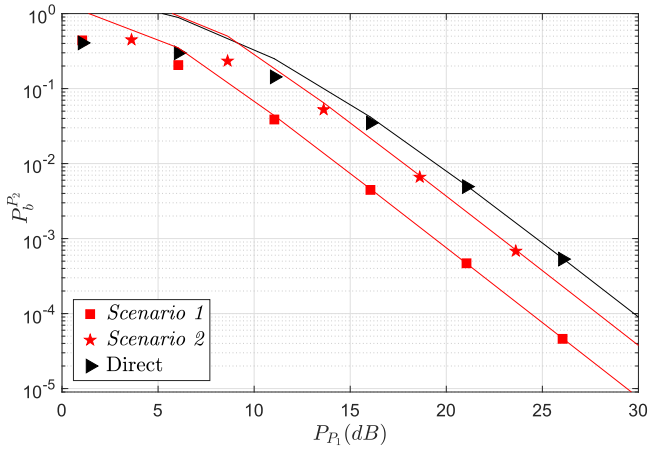

Fig. 4. BEP performance of P_2 when $M_P = M_S = N_t^P = N_t^S = 4$.

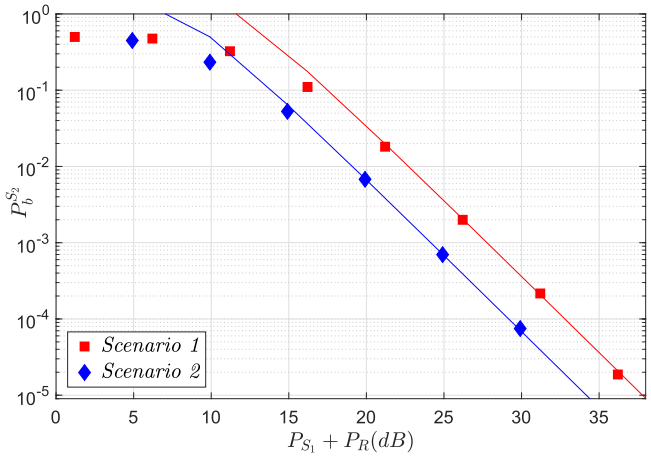

Fig. 5. BEP performance of S_2 for $M_P = M_S = N_t^P = N_t^S = 4$.

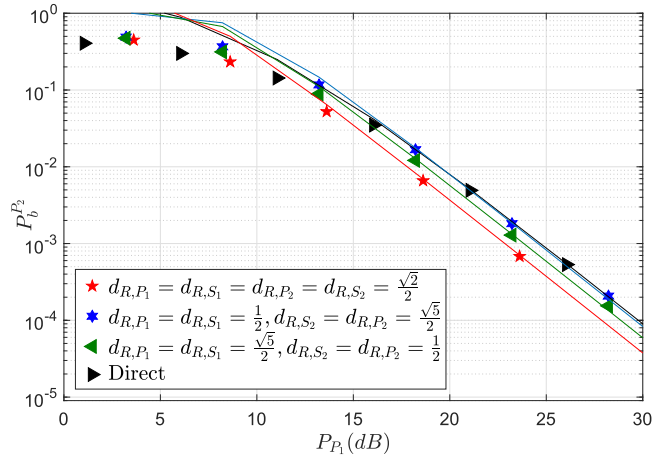

Fig. 6. The effect of the relay position on the BEP performance of P_2 for $M_P = M_S = N_t^P = N_t^S = 4$ and *Scenario 2*.

B. Bit Error Rate

In this section, the bit error performances are evaluated by considering the system configuration in 2-D and 3-D plane. The OPA parameters given in Tables are considered. In all figures, straight lines and markers represent theoretical and simulation curves, respectively. In Figs. 4–6, system configuration is considered in 2-D plane and OPA parameters given in Table III are adopted.

In Fig. 4, the BEP performance of P_2 is provided to compare *Scenarios 1* and *2* with the direct transmission between P_1 and P_2 when $M_P = M_S = N_t^P = N_t^S = 4$ and $d_{\mathrm{R,P_1}} = d_{\mathrm{R,S_1}} = d_{\mathrm{R,P_2}} = d_{\mathrm{R,S_2}} = \sqrt{2}/2$. *Scenario 1* provides the best BEP performance for P_2 as expected, which provides a BER value of 10^{-5} at about 29.5 dB. However, the BEP performance becomes worse, when *Scenario 2* is adopted and it provides the same BER value at 32.7 dB. Note that both scenarios exhibit better performance compared to that of direct transmission.

In Fig. 5, the BEP performance of SU is given for *Scenarios 1* and *2*, when $M_P = M_S = N_t^P = N_t^S = 4$ and $d_{\mathrm{R,P_1}} = d_{\mathrm{R,S_1}} = d_{\mathrm{R,P_2}} = d_{\mathrm{R,S_2}} = \sqrt{2}/2$. The best BEP performance is achieved by *Scenario 2* for SU, which provides a BER value of 10^{-5} at 34 dB while *Scenario 1* reaches this value at 37.8 dB. Therefore, adopting *Scenario 2* provides fair solutions for both user pairs.

In Fig. 6, the effect of the relay position on the BEP performance of P_2 is depicted for *Scenario 2* by moving R through the vertical direction from the midst of P_1 and S_1 to the midst of P_2 and S_2 when $M_P = M_S = N_t^P = N_t^S = 4$. The best bit error performance is provided when the relay is equidistant to all sources. When R moves to the midst of P_2 and S_2, the performance becomes worse; however, a better performance compared to the direct transmission between P_1 and P_2 is obtained. If R is in the midst of P_1 and S_1, the performance is equivalent to the direct link, which does not provide any improvement in terms of PU. For example, it provides a BER value of 10^{-4} for P_2 at 28 dB, when R is equidistant to all sources, while the direct transmission provides the same BER value at 29.8 dB.

In Figs. 7 and 8, the proposed protocol is compared with a four-time-slot reference scheme in terms of BEP performance of PUs and SUs by considering system configuration in 3-D plane. In the reference scheme, during the first and second time slots, PUs and SUs transmit their SM symbols to the relay and the relay applies PLNC, respectively. In the third (fourth) time slot, R transmits the PLNC mapped SM symbol of PUs (SUs) to PUs (SUs). Due to the use of an additional time slot compared to our protocol, R consumes $P_{\mathrm{R}}/2$ power per time slot to limit the total power consumed by relay to P_{R}. Moreover, since the reference scheme is a four-time-slot system, and *Scenario 1* considers only minimizing the BEP of primary user pair, it allocates the whole of the available power to P_1 and P_2 for the reference scheme. Therefore, it would be pointless to compare the reference and proposed schemes under *Scenario 1*. For *Scenario 2*, symmetric data rates for PU and SU pairs are

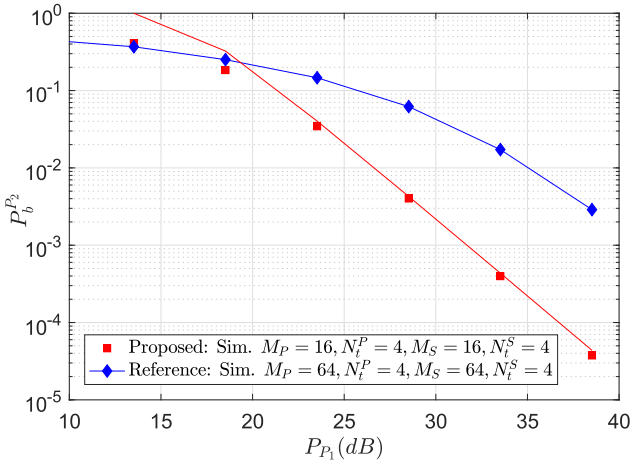

Fig. 7. BER performance comparison of P_2 for *Scenario 2*.

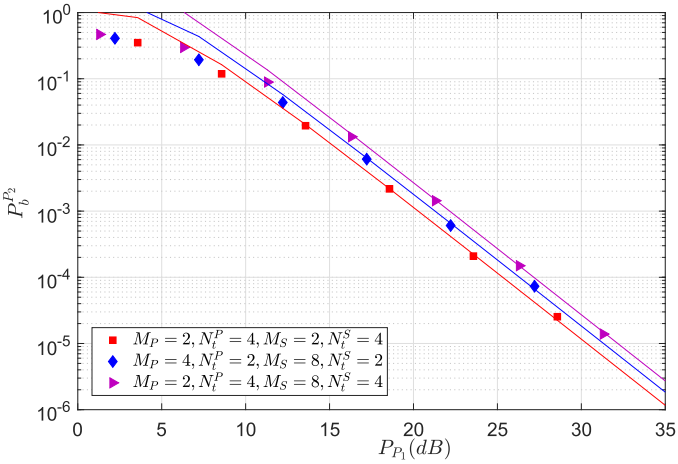

Fig. 9. BER performance of P_2 for *Scenario 2*

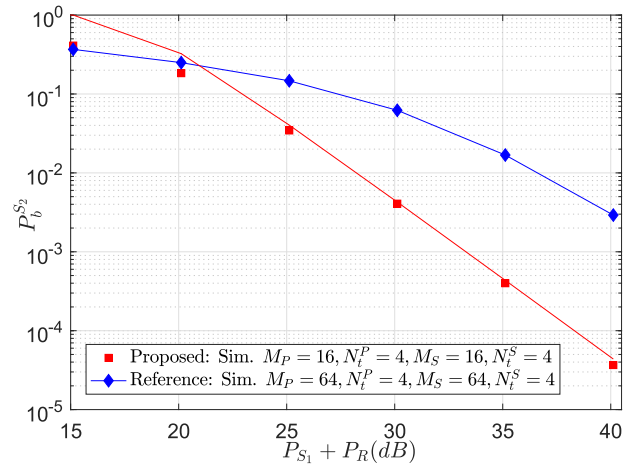

Fig. 8. BER performance comparison of S_2 for *Scenario 2*.

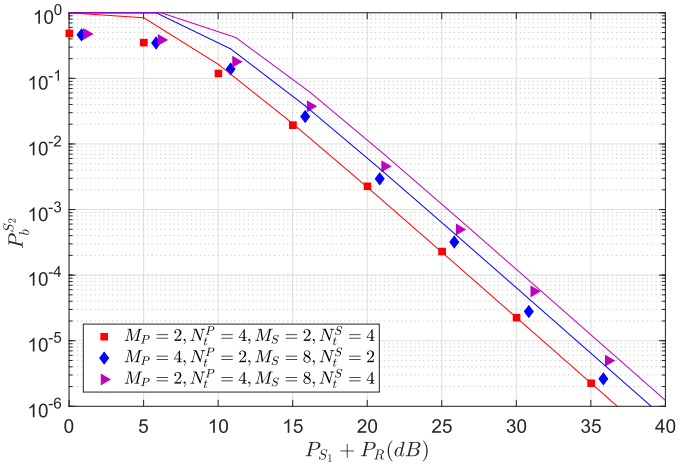

Fig. 10. BER performance of S_2 for *Scenario 2*

considered when $M_P = M_S = M$ and $N_t^P = N_t^S = N_t$. To make comparisons under the same spectral efficiency, the parameter values of $M = 16, N_t = 4$ and $M = 64, N_t = 4$ are chosen for our scheme and the reference scheme, respectively. Since it is more difficult to increase the number of transmit antennas in practice, the number of transmit antennas are assumed to be equal, while modulation orders are varied for these two protocols. The distances are taken as $d_{\mathrm{R,P_1}} = d_{\mathrm{R,P_2}} = d_{\mathrm{R,S_1}} = d_{\mathrm{R,S_2}} = d_{\mathrm{P_1,S_1}} = d_{\mathrm{P_1,S_2}} = d_{\mathrm{P_2,S_1}} = d_{\mathrm{P_2,S_2}} = 1$. OPA parameters are adopted as $\beta = 0.9$ and $\alpha = 0.5$, for both schemes. Note that, for the same spectral efficiencies, there is not much difference between the OPA parameters of the proposed protocol and the reference scheme. In Fig. 7, the BER performances of the proposed protocol and the reference scheme are given for PU pair under equal spectral efficiency. For high values of $P_{\mathrm{P_1}}$, the proposed protocol provides better BER performance than the reference scheme. For example, the proposed protocol provides a BER value of 3×10^{-3} at 29.3 dB, while the reference scheme provides this value at 38.4 dB. In Fig. 8, the BER performances of proposed protocol and the reference scheme in terms of SU pair are given under the same spectral efficiency. As expected, the proposed protocol gives a BER value of 3×10^{-3} at 30.9 dB while the reference scheme reaches this value at 40 dB. From Figs. 7 and 8, it can be concluded that the proposed protocol outperforms the reference scheme in terms of BER performance at high data rates.

TABLE IV
PARAMETERS (β_0, α_0) FOR $d_{\mathrm{R,P_1}} = d_{\mathrm{R,P_2}} = d_{\mathrm{R,S_1}} = d_{\mathrm{R,S_2}} = \sqrt{2}/2$ AND $d_{\mathrm{P_1,S_1}} = d_{\mathrm{P_1,S_2}} = d_{\mathrm{P_2,S_1}} = d_{\mathrm{P_2,S_2}} = 1$

M_P	N_t^P	M_S	N_t^S	*Scenario 2*
2	4	2	4	(0.91, 0.5)
4	2	8	2	(0.9, 0.37)
2	4	8	4	(0.9, 0.3)

In Figs. 9 and 10, BER performance of PUs and SUs for different rates and *Scenario 2* are provided, where the OPA parameters given in Table IV are considered. For example, in Fig. 9, a BER value of 10^{-5} is reached at 30.3 dB when $M_P = 2, N_t^P = 4, M_S = 2, N_t^S = 4$ while for $M_P = 2$, $N_t^P = 4, M_S = 8, N_t^S = 4$, this value is reached at 32.2 dB.

It can be concluded similarly from Fig. 10 that when the data rate increases, BER performance degrades, as expected.

VI. Conclusion

In this paper, a bidirectional cognitive cross network design utilizing SM along with PLNC has been considered, where OPA is adopted. Considerable gains in power consumption have been obtained with respect to the equivalent reference systems. The effect of the relay position on the BEP performance of P_2 is also investigated. The best BEP performance of P_2 has been reached when the relay is equidistant to all other nodes. As a future work, energy harvesting relaying through multiple access channels at the first and the second time slots can be considered, which seems to be a promising approach to the proposed bidirectional cognitive cross network design, in terms of power efficiency.

References

[1] M. E. Tanab and W. Hamouda, "Resource allocation for underlay cognitive radio networks: A survey," *IEEE Commun. Surveys Tut.*, vol. 19, no. 2, pp. 1249–1276, Second Quarter 2017.

[2] A. Ali and W. Hamouda, "Advances on spectrum sensing for cognitive radio networks: Theory and applications," *IEEE Commun. Surveys Tut.*, vol. 19, no. 2, pp. 1277–1304, Second Quarter 2017.

[3] W. Liang, S. X. Ng, and L. Hanzo, "Cooperative overlay spectrum access for cognitive radio networks," *IEEE Commun. Surveys Tut.*, vol. 19, no. 3, pp. 1924–1944, Third Quarter 2017.

[4] S. C. Liew, S. Zhang, and L. Lu, "Physical-layer network coding: Tutorial, survey, and beyond," *Phys. Commun.*, vol. 6, pp. 4–42, 2013.

[5] J. He and S. C. Liew, "Building blocks of physical-layer network coding," *IEEE Trans. Wireless Commun.*, vol. 14, no. 5, pp. 2711–2728, May 2015.

[6] A. Thampi, S. C. Liew, S. Armour, Z. Fan, L. You, and D. Kaleshi, "Physical-layer network coding in two-way heterogeneous cellular networks with power imbalance," *IEEE Trans. Veh. Technol.*, vol. 65, no. 11, pp. 9072–9084, Nov. 2016.

[7] M. D. Renzo, H. Haas, and P. M. Grant, "Spatial modulation for multiple-antenna wireless systems: A survey," *IEEE Commun. Mag.*, vol. 49, no. 12, pp. 182–191, Dec. 2011.

[8] Y. Zhou, H. Zhang, D. Yuan, P. Zhang, and H. Liu, "Differential spatial modulation with BPSK for two-way relay wireless communications," *IEEE Commun. Lett.*, vol. 21, no. 6, pp. 1361–1364, Jun. 2017.

[9] S. Guo, H. Zhang, P. Zhang, and D. Yuan, "Adaptive mapper design for spatial modulation with lightweight feedback overhead," *IEEE Trans. Veh. Technol.*, vol. 66, no. 10, pp. 8940–8950, Oct. 2017.

[10] S. Guo, H. Zhang, P. Zhang, D. Wu, and D. Yuan, "Generalized 3-D constellation design for spatial modulation," *IEEE Trans. Commun.*, vol. 65, no. 8, pp. 3316–3327, Aug. 2017.

[11] A. Afana, T. M. N. Ngatched, O. A. Dobre, and S. Ikki, "Cooperative DF cognitive radio networks with spatial modulation with channel estimation errors," in *Proc. IEEE Wireless Commun. Netw. Conf.*, San Francisco, CA, USA, 2017, pp. 1–5.

[12] Z. Bouida, A. Ghrayeb, and K. A. Qaraqe, "Adaptive spatial modulation for spectrum sharing systems with limited feedback," *IEEE Trans. Commun.*, vol. 63, no. 6, pp. 2001–2014, Jun. 2015.

[13] S. Üstünbaş, E. Basar, and U. Aygölü, "Cooperative spectrum sharing protocol using spatial modulation," *IET Commun.*, vol. 11, no. 11, pp. 1759–1767, Sep. 2017.

[14] S. Üstünbaş, E. Basar, and Ü. Aygölü, "Cognitive cross network design with physical-layer coding and spatial modulation," *Electron. Lett.*, vol. 53, no. 6, pp. 432–434, 2017.

[15] M. K. Simon and M.-S. Alouini, *Digital Communication over Fading Channels*. Hoboken, NJ, USA: Wiley, 2005.

[16] R. Mesleh, O. Hiari, A. Younis, and S. Alouneh, "Transmitter design and hardware considerations for different space modulation techniques," *IEEE Trans. Wireless Commun.*, vol. 16, no. 11, pp. 7512–7522, Nov. 2017.

Seda Üstünbaş received the B.S.(Hons.) degree from Istanbul University, Istanbul, Turkey, in 2013, and the M.S. degree from Istanbul Technical University, Istanbul, Turkey, in 2017. She is currently working toward the Ph.D. degree and a Member of Wireless communication laboratory, Istanbul Technical University. Her research interests include MIMO systems, cooperative communications, cognitive radio, index modulation, nonorthogonal multiple access and energy harvesting. She was a TPC member for several IEEE conferences and as a reviewer for IEEE journals.

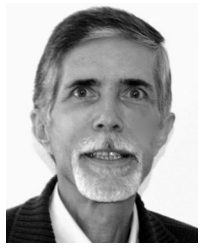

Ümit Aygölü received the B.S., M.S., and Ph.D. degrees all in electrical engineering from Istanbul Technical University, Istanbul, Turkey, in 1978, 1984, and 1989, respectively. From 1980 to 1986, he was a Research Assistant and a Lecturer from 1986 to 1989, with Yildiz Technical University, Istanbul, Turkey. In 1989, he became an Assistant Professor with Istanbul Technical University where he became an Associate Professor and Professor in 1992 and 1999, respectively. His current research interests include MIMO systems, cooperative communications, cognitive radio, energy harvesting, and spatial modulation.

Ertugrul Basar (S'09–M'13–SM'16) received the B.S.(Hons.) degree from Istanbul University, Istanbul, Turkey, in 2007, and the M.S. and Ph.D. degrees from Istanbul Technical University, Istanbul, Turkey, in 2009 and 2013, respectively.

From 2011 to 2012, he was with the Department of Electrical Engineering, Princeton University, Princeton, NJ, USA, as a visiting research collaborator. He was an Assistant Professor with Istanbul Technical University from 2014 to 2017, where he is currently an Associate Professor of Electronics and Communication Engineering. He is an inventor of three pending/granted patents on index modulation schemes. His primary research interests include MIMO systems, index modulation, cooperative communications, OFDM, and visible light communications. Recent recognition of his work includes the Young Scientists Award of the Science Academy (Turkey) in 2018, the Turkish Academy of Sciences Outstanding Young Scientist Award in 2017, the first-ever IEEE Turkey Research Encouragement Award in 2017, and the Istanbul Technical University Best Ph.D. Thesis Award in 2014. He is also the recipient of four Best Paper Awards including one from the IEEE International Conference on Communications 2016. He was a TPC member for several IEEE conferences and is a regular reviewer for various IEEE journals. He is currently an Associate Editor of the IEEE Communications Letters and the IEEE Access, and as an Editor of *Physical Communication* (Elsevier).